Environmental Science and Pollution Research
https://doi.org/10.1007/s11356-021-14918-y

RESEARCH ARTICLE

Carbon nanotubes from waste cooking palm oil as adsorbent materials for the adsorption of heavy metal ions

Suriani Abu Bakar[1,2] · **Norhafizah Jusoh**[1,2] · **Azmi Mohamed**[1,3] · **Muqoyyanah Muqoyyanah**[1,2] · **Mohd Hafiz Dzarfan Othman**[4] · **Mohamad Hafiz Mamat**[5] · **Mohd Khairul Ahmad**[6] · **Mohd Ambri Mohamed**[7] · **Muhammad Noor Azlan**[2] · **Norhayati Hashim**[3] · **Muhammad Danang Birowosuto**[8] · **Tetsuo Soga**[9]

Received: 31 October 2020 / Accepted: 10 June 2021

Abstract

In this work, waste cooking palm oil (WCPO)-based carbon nanotubes (CNTs) with encapsulated iron (Fe) nanoparticles have been successfully produced via modified thermal chemical vapor deposition method. Based on several characterizations, the dense WCPO-based CNT was produced with high purity of 89% and high crystallinity proven by low I_D/I_G ratio (0.43). Moreover, the ferromagnetic response of CNTs showed that the average coercivity and magnetization saturation were found to be 551.5 Oe and 13.4 emu/g, respectively. These produced WCPO-based CNTs were further used as heavy metal ions adsorbent for wastewater treatment application. Some optimizations, such as the effect of different adsorbent dosage, varied initial pH solution, and various heavy metal ions, were investigated. The adsorption studies showed that the optimum adsorbent dosage was 1.8 g/L when it was applied to 100 mg/L Cu (II) solution at neutral pH (pH 7). Further measurement then showed that high Cu (II) ion removal percentage (~80%) was achieved when it was applied at very acidic solution (pH 2). Last measurement confirmed that the produced WCPO-based CNTs successfully removed different heavy metal ions in the following order: Fe (II) > Zn (II) ≈ Cu (II) with the removal percentage in the range of 99.2 to 99.9%. The adsorption isotherm for Cu (II) was better fitted by Langmuir model with a correlation coefficient of 0.82751. WCPO-based CNTs can be a potential material to be applied as adsorbent in heavy metal ion removal.

Keywords Adsorbent · Carbon nanotubes · Chemical vapor deposition · Coercivity · Heavy metal ions · Magnetic

---

Responsible Editor: Tito Roberto Cadaval Jr

✉ Suriani Abu Bakar
absuriani@yahoo.com

[1] Nanotechnology Research Centre, Perak, Malaysia

[2] Department of Physics, Universiti Pendidikan Sultan Idris, Perak, Malaysia

[3] Department of Chemistry, Faculty of Science and Mathematics, Universiti Pendidikan Sultan Idris, 35900 Tanjung Malim, Perak, Malaysia

[4] Advanced Membrane Technology Research Centre (AMTEC), Universiti Teknologi Malaysia, 81310 Skudai, Johor, Malaysia

[5] NANO-ElecTronic Centre (NET), Faculty of Electrical Engineering, Universiti Teknologi MARA (UiTM), 40450 Shah Alam, Selangor, Malaysia

[6] Microelectronic and Nanotechnology-Shamsuddin Research Centre (MiNT-SRC), Faculty of Electrical and Electronic Engineering, Universiti Tun Hussein Onn Malaysia, Parit Raja, Malaysia

[7] Institute of Microengineering and Nanoelectronics (IMEN), Universiti Kebangsaan Malaysia, 43600 Bangi, Selangor, Malaysia

[8] CNRS International NTU Thales Research Alliance (CINTRA), Research Techno Plaza, 50 Nanyang Drive, Border X Block, Singapore 637553, Singapore

[9] Department of Frontier Materials, Nagoya Institute of Technology, Gokiso-cho, Showa-ku, Nagoya 466-8555, Japan

Introduction

At present, water pollution is one of the greatest challenges in our time. The lack of fresh and clean water is the main problem around the world. Water contamination by heavy metals has become more serious with increased industrial activities such as metallurgical, chemical manufacturing, tannery, battery manufacturing industries, and others, as well as rapid urbanization (Ahmad et al. 2009; Božić et al. 2009; Sankhla et al. 2016). Meanwhile, the improper disposal and discharge of used oil, such as waste engine oil (WEO) to the environment, also contributes to heavy metal contamination of water. As an example, the high concentration of heavy metals, such as iron (Fe), zinc (Zn), copper (Cu), and others, in WEO can be poisonous to our ecological system and human health (Suriani et al. 2015a). WEO can percolate into groundwater or rivers, which may be used as water source for cooking, drinking, and others. The United States Environmental Protection Agency provided the guidelines for the limit value of heavy metals in the drinking water for Cu, Fe, and Zn of 1.3, 0.3, and 0.5 mg/L, respectively (Fernández-Luqueño et al. 2013). Higher concentration of Cu, which is frequently observed in surface water, can affect human health, causing kidney failure, system irritation, depression, anemia, Alzheimer's, Parkinson's, and other illnesses (Ahmad et al. 2009; Briffa et al. 2020). Excessive exposure to Fe and Zn through water ingestion results in its accumulation in the muscle, liver, and gills (Fernández-Luqueño et al. 2013; Briffa et al. 2020). Therefore, the removal of heavy metals from water is considered the main issue at present. Various techniques, such as reverse osmosis, adsorption, chemical precipitation, ion-exchange, electrodialysis, and solvent extraction, have been explored for the removal of these heavy metals from polluted water (Malik et al. 2019). However, when the concentrations of heavy metal ions are raised to 500 mg/L, these techniques become ineffective and uneconomical, with permissible limits of heavy metal ions in solution of only approximately 1 mg/L (Ahmad et al. 2009; Balintova et al. 2012). Given the aspects of economy and effectiveness, the adsorption process is considered one of the promising and widely used methods for solving these problems (Siddiqa et al. 2015; Adeli et al. 2017).

Numerous adsorbent materials, such as activated carbon (Gangupomu et al. 2016), peat (Chwastowski et al. 2017; Bartczak et al. 2018), biomaterials (Gao et al. 2017), rice husk (Amen et al. 2020; Nata et al. 2020), peanut hulls (Shan et al. 2020), zeolites (Oliveira et al. 2019), chitosan (Liu et al. 2019), and functionalized polymers (Liu et al. 2020), are reported to be capable of functioning as adsorbent materials for the removal of heavy metals from aqueous solutions. However, most of these adsorbent materials show lower adsorption capacity owing to the limitation of active sites, difficulties in the separation of adsorbent from solution, expensive production cost, and complicated methodology, such as functionalization of adsorbents (Zare et al. 2015; Gangupomu et al. 2016). On account of high surface area, high adsorption capacity, and rapid separation from the solution, carbon nanotubes (CNTs) have been explored to remove heavy metal ions in solution or wastewater (Yadav and Srivastava 2017; Duan et al. 2020; Wadhawan et al. 2020). Owing to their tunable physical, electrical, structural, and chemical properties, CNTs can inspire innovative and promising technologies to solve water shortage and pollution problems (Ihsanullah et al. 2016). Liu and Cheng (2005) and Pyrzyńska and Bystrzejewski (2010) reported the removal of heavy metal ions from aqueous solutions by using CNT-based fossil fuel as adsorbent material. CNTs are relatively expensive, with the current price being approximately \$25–100 per gram by using fossil fuel-based carbon sources (Lu et al. 2007). Therefore, cost is frequently a limiting factor for large-scale applications of CNT-based materials for water treatment. In overcoming this problem, high-quality CNTs were successfully synthesized by using free carbon sources, such as WEO, waste cooking palm oil (WCPO), waste chicken fat, and gutter oil (Suriani et al. 2010, 2013, 2015a, b, c, 2016a, c), by thermal chemical vapor deposition (TCVD) method, which is a cost-effective approach for large-scale CNT production (Suriani et al. 2009, 2016b; Shamsudin et al. 2012).

Ordinary CNTs encounter problems, such as difficulty in dispersion and separation in aqueous solution because of small particle size (Huang et al. 2015; Rodríguez et al. 2020). Hence, the combination of the magnetic behavior of metal oxides with CNTs as adsorbent materials enhances the adsorption of heavy metals in wastewater. During adsorption, CNTs can be well dispersed in water for the removal of heavy metal ions. Qu et al. (2008) developed CNTs filled with Fe_2O_3 particles for the removal of heavy metal ions from aqueous solutions. Tang et al. (2012) reported magnetic CNTs as adsorbent materials for the simultaneous removal of heavy metal ion Cu (II) and atrazine from aqueous solution. However, the method involved certain modification and functionalization for the production of magnetic CNTs. Current methods for the synthesis of magnetic CNTs present several disadvantages, such as high cost, time consumption, environmental toxicity, complicated methodology, and low yield (Wright et al. 2012; Bollen et al. 2016; Sengupta 2018). Hence, the introduction of a metal catalyst by TCVD is the simplest technique to produce CNTs with filled metal nanoparticles. As seen from a previous work (Suriani et al. 2013, 2015a, c, 2016a, b, c), the encapsulated Fe nanoparticles in CNTs were achieved using ferrocene as catalyst. Fe particles were continuously supplied by decomposition of ferrocene during CNT growth, which may result in longer Fe nanoparticles encapsulated in the CNT tubes (Liu et al. 2010; Sengupta 2018).

To the best of our knowledge, CNTs from waste, such as WCPO, have yet to be systematically studied as adsorbent material for the removal of heavy metal ions. Here, we reported the high production of CNTs by modified TCVD and using ferrocene as catalyst and WCPO as carbon source (Suriani et al. 2016b) for the application in water treatment. We find that Fe nanoparticle-encapsulating CNT tubes are good adsorbent materials for the removal of heavy metal ions. The prepared CNTs were used as adsorbent materials for the removal of Fe (II), Zn (II), and Cu (II). Meanwhile, the effects of adsorbent dosage and changes in pH were studied. We also proposed the adsorption mechanism of heavy metal ions by using WCPO-based CNTs as adsorbent materials.

Experimental and method

Synthesis of adsorbent material CNTs from WCPO

The synthesis of CNTs was similar to that in a previous report (Suriani et al. 2010). The precursor container was filled with 1000 mL WCPO and 5.33 wt% ferrocene as the catalyst and then connected to the peristaltic sprayer. Then, the precursor was sprayed into the furnace at a flow rate of 30 mL/min and 15 min of time interval between sprayers. The precursor furnace and deposition furnace were set at 500 and 800 °C, respectively. After synthesis, a WCPO-based CNT powder was collected in the collection container at the end of the deposition furnace (Suriani et al. 2016b). The WCPO-based CNT sample was then analyzed by using field-emission scanning electron microscopy (FESEM) (Hitachi SU8020), micro-Raman spectroscopy (Renishaw InVia microRaman system), and thermogravimetric analysis (TGA) (Mettler Toledo TGA/DSC 1 STAR^{e} System). The magnetic properties of the produced WCPO-based CNTs were determined using a vibrating sample magnometer (VSM) (LakeShore Model 7404) at room temperature. The as-synthesized CNTs were then used as adsorbent material for application in the removal of heavy metal ions.

Adsorption experiments

Analytical-grade chloride salt solutions (Merck) were used to prepare the stock solution containing 1000 mg/L of Cu (II), Zn (II), and Fe (II) heavy metal ion. To obtain the required concentrations, metal chloride salts were diluted with deionized water. In this study, the initial concentration of heavy metal ions was set to 100 mg/L for all batch adsorption experiments. To study the effect of adsorbent dosage on heavy metal ions adsorption, a total of 0.2–2.2 g of CNTs from WCPO were dispersed in a 250 mL solution containing 100 mg/L of Cu (II), and then, the mixture was stirred for 1 h at room temperature. The investigation of pH solution effect was then carried out by varying Cu (II) pH solution of 1–6. The acidic solution was adjusted by using a 1 M HCl solution. Meanwhile, the variation in heavy metal ions Cu (II), Zn (II), and Fe (II) was studied using 100 mg/L initial concentration at pH 7. After the adsorption process, WCPO-based CNTs were separated from the solution by filtration process. The concentration of remaining heavy metal ions in the solution was analyzed using inductively coupled plasma atomic emission spectroscopy (ICP-OES) (Agilent Technologies 700 series). The functional groups of CNTs from WCPO before and after adsorption of heavy metal ions were determined using Fourier transform infrared spectroscopy (FTIR) (Thermo Nicolet 6700). Meanwhile, trace amounts of heavy metal ions in the CNTs after adsorption process were analyzed using energy dispersive X-ray spectrometer (EDS) and FESEM. The removal percentage of heavy metal ions and equilibrium adsorption capacity were calculated based on the following equations:

$$\%Removal = \frac{(C_o - C_e)}{C_o} \times 100 \tag{1}$$

$$q_e = \frac{(C_o - C_e)\ V}{m} \tag{2}$$

where C_o and C_e are the initial and equilibrium heavy metal ion concentration (mg/L), respectively; q_e is the equilibrium adsorption capacity (mg/g); and V and m are the volume of the solution (L) and adsorbent dosage (g), respectively (Shan et al. 2020).

Results and discussion

Characterization of WCPO-based CNTs as adsorbent material

Figure 1a, b presents FESEM images of the synthesized WCPO-based CNTs. The synthesized CNTs possess a small diameter between 15.3 and 32.7 nm and are denser than those in the previous study (Suriani et al. 2016b). HRTEM of the sample in Fig. 1c indicates that CNTs consist of approximately 20 graphitic layers with interlayer spacing of 0.33 nm, which is consistent with graphite interplanar spacing (Suriani et al. 2015b, 2016b). The HRTEM image in Fig. 1d reveals that Fe nanoparticle of 90 nm in length was encapsulated at the middle of the nanotube with inner and outer diameters of 9.8 and 26.7 nm, respectively. The TEM image (Fig. 1e) further confirmed that most of the Fe catalysts were encapsulated in the nanotube (shown by red arrow) and were responsible for the magnetic properties of CNTs.

The representative hysteresis loop of as-prepared CNTs (Fig. 1f) shows a smooth S-shaped curves symmetric around $H = 0$, which exhibits a typical ferromagnetic behavior. The

Fig. 1 **a**–**b** FESEM, **c**–**e** HRTEM images, **f** VSM analysis, **g** micro-Raman spectrum, and **h** TGA and DTA curves of the produced WCPO-based CNTs

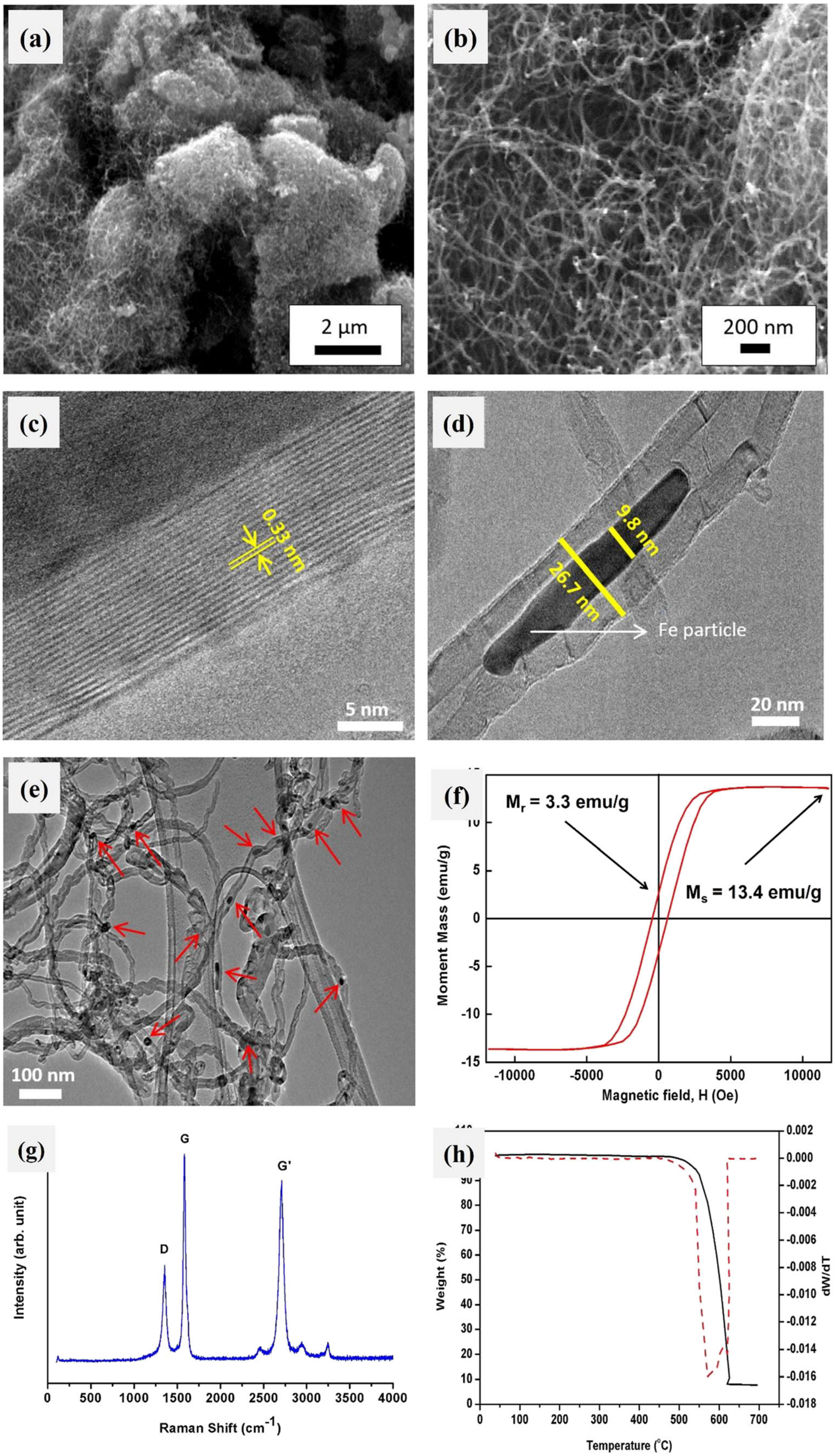

saturation magnetization (M_s) and coercivity value of the sample are about 13.4 emu/g and 551.5 Oe, respectively. This M_s value was comparable than those reported by Fu et al. (14.1 emu/g) and Ahangari et al. (15 emu/g) which synthesized Fe_3C-filled aligned CNTs and zinc nickel ferrite-CNTs nanocomposite, respectively (Fu et al. 2013; Ahangari et al. 2019). The ratio of remnant to saturation magnetization, M_r/M_s of prepared sample, was found to be 0.25, as is in good agreement with the ferromagnetic character of the material ($M_r/M_s = 0.25–0.30$) (Luo et al. 2010). The magnetic character of the synthesized CNTs was believed to be due to the presence of Fe nanoparticles in the nanotubes. These nanoparticles act as catalyst in CNT growth. Owing to this magnetic character, CNTs from WCPO can be utilized as adsorbent material for heavy metal ion removal. The function of magnetic nanoparticle encapsulated in the adsorbent material allows the material to be easily dispersed in aqueous solution (Wang et al. 2012; Li et al. 2013; Sun et al. 2014) and enhance the capacity of adsorption of metal ions in acidic solution (Vázquez et al. 2016).

The micro-Raman spectrum of the WCPO-based CNTs is represented in Fig. 1g. Two intense peaks of D- and G-peaks were observed at around 1351 and 1581 cm^{-1}, respectively. Sharp G-peak indicates the well-graphitized WCPO-based CNT formation which is in good agreement with the HRTEM analysis. The I_D/I_G ratio of the WCPO-based CNTs was found to be 0.43, indicated the good crystallinity of WCPO-based CNTs (Suriani et al. 2015b). Meanwhile, the intense G'-peak at 2698 cm^{-1} indicated the smaller diameter with low defect of the produced CNTs. The presence of low defect may decrease the electrical resistivity of CNTs and lead to the increase in the adsorption of heavy metal ions onto the CNT surface (Lu et al. 2006).

The TGA and differential TGA (DTGA) curves of the WCPO-based CNTs are presented in Fig. 1h. Small weight loss of 2.3% detected at around 490–550 °C was mainly due to the decomposition of amorphous carbon. No significant weight loss was found between 250 and 500 °C, which demonstrates better crystallinity degree of nanotubes with minimal amorphous carbon content (Suriani et al. 2009, 2015b). At a temperature of 510 °C, the oxidation of WCPO-based CNTs was started and then followed by the combustion of WCPO-based CNTs at temperature of 571 °C as indicated by the exothermic peak in the DTGA curve. The remaining 8.1% of the total weight loss was due to the presence of the Fe catalyst as confirmed by HRTEM and other volatile materials in the sample. The purity of the WCPO-based CNTs was found to be 89.6%, which demonstrates high sample purity (Suriani et al. 2015b). Hence, CNT from WCPO is believed to be the best candidate as adsorbent material for the removal of heavy metal ions owing to the low amorphous carbon and impurities present in the sample as confirmed by Raman spectroscopy and TGA.

Effect of adsorbent dosage

The effect of WCPO-based CNT dosage on the removal percentage of Cu (II) is studied at the initial concentration and pH of 100 mg/L and 7, respectively. The results reveal that by increasing WCPO-based CNT dosage from 0.2 to 1.6 g/L, higher Cu (II) removal percentage from 28.1 to 98.0% was achieved as shown in Fig. 2. Higher adsorbent dosage increases the number of active sites and yields greater availability of exchangeable sites between WCPO-based CNTs and Cu (II) in the solution (Kosa et al. 2012; Bernard and Jimoh 2013; Sun et al. 2014; Mubarak et al. 2015; Vázquez et al. 2016; Gupta et al. 2017; Ahangari et al. 2019). Further increments of CNT dosage from 1.6 to 2.2 g/L did not significantly affect the Cu (II) removal percentage, with the removal of Cu remaining in the range of ~98.0% prior to saturation at 99.0% at 1.8–2.2 g/L CNTs. All Cu (II) ions are assumed to be attached at the active sites of 1.8 g CNTs. Hence, in this study, the optimum dosage of CNTs was ~1.8 g/L to remove ~99% of Cu (II) at the initial concentration of 100 mg/L. The study of adsorbent dosage is in good agreement with the findings of Mubarak et al. which reported that up to ~96% of Cu (II) ions were successfully removed from the solution by using 0.05–0.10 g of MWCNTs at a low initial concentration of 10 mg/L (Mubarak et al. 2015).

The percentage of Cu (II) removal was seen to be highly dependent on the initial concentration of the solution, where the removal percentage of Cu (II) decreases with the increase in initial concentration of Cu (II) (Rao et al. 2009). From the observation in our current work, at 0.2 g/L adsorbent dosage of WCPO-based CNTs, only ~28% of Cu (II) ions were removed from the solution by consuming high initial concentration of 100 mg/L. In contrast to the studies reported by Kosa

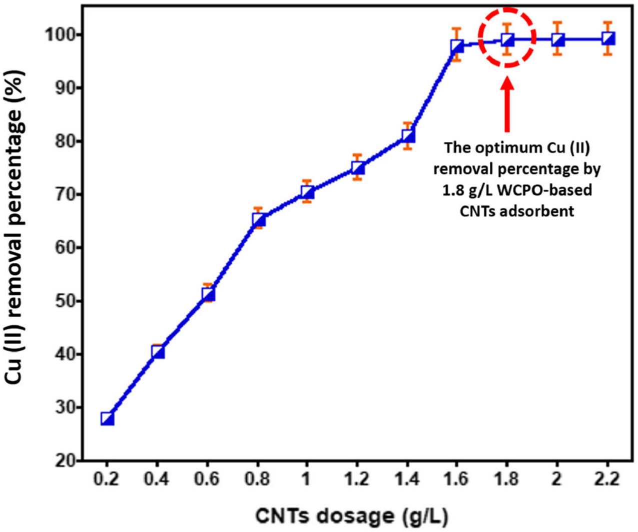

Fig. 2 Removal percentage of Cu (II) by using 0.2–2.2 g WCPO-based CNTs as adsorbent with initial pH and concentration of 7 and 100 mg/L, respectively

et al. (Kosa et al. 2012), the same MWCNT dosage of 0.2 g and almost the entire (~98%) Cu (II) amount were successfully removed at an initial concentration of 1 mg/L. The lack of available active sites for further adsorption of metal ions on the adsorbent surface hinders further adsorption of heavy metal ions in the solution. Thus, a high adsorbent dosage is needed to provide adequate active sites to enhance the adsorption of metal ions at high initial concentration (Rao et al. 2009; Ma et al. 2012).

Therefore, for confirmation, further investigation using low initial concentration of Cu (II) solution of 10 mg/L was conducted with 0.05 to 0.10 g/L WCPO-based CNTs as adsorbent. The results reveal that up to ~99% of Cu (II) ions were successfully removed from the solution by 0.10 g/L WCPO-based CNTs. The good adsorption of metal ions at low initial concentration was also believed to be due to the high collision efficiency between heavy metal ions and the WCPO-based CNT adsorbent, leading to better adsorption capacity toward metal ions particularly at low initial concentration (Ma et al. 2012). In the meantime, this finding was superior to that in the work reported by Mubarak et al. (Mubarak et al. 2015), where only ~96% Cu (II) ions were removed using the same MWCNT dosage of 0.10 g.

In comparison with other adsorbents based on waste materials, such as activated carbon from orange peel (ACOP), maple, Meranti, and fir sawdust, CNTs from WCPO have shown considerable potential as low-cost absorbent materials owing to the ability to adsorb metal ions at lower dosage (Bernard and Jimoh 2013; Vázquez et al. 2016). With ACOP as an adsorbent material example, only 50–61% Cu (II) was removed by 0.1–1.0 g of ACOP dosage at an initial concentration of Cu (II) of ~43 mg/L (Bernard and Jimoh 2013). In comparison, CNTs from WCPO prepared in this study successfully removed ~99% of Cu (II) by 1.8 g/L at an initial solution concentration of 100 mg/L. Meanwhile, substantial amounts of 10 g maple and Meranti and 5 g fir tree sawdust were only capable of removing about ~72–89% Cu (II) at initial concentrations of 50, 100, and 48 mg/L, respectively (Rafatullah et al. 2009; Rahman and Islam 2009; Marković et al. 2011). BET and Langmuir analysis of 34.418 and 55.698 m^2/g, respectively presented by previous report, also confirmed the large specific surface area of the produced WCPO-based CNTs (Maryam et al. 2013). This value also in a good agreement with Peigney et al. (2001) which reported that smaller-sized CNTs (refers to the tube diameter size of ~30 nm) possessed high surface area of 25–50 m^2/g thus provided higher available specific surface of CNTs (refer to Fig. 1d) to enhance metal ion adsorption (Marković et al. 2011). Meanwhile, adsorbent materials derived from natural waste that are used as adsorbent materials, such as ACOP, maple, Meranti, and fir tree sawdust, present drawbacks, such as larger average particle size in the range of 100–600 μm, which is attributed to low adsorption capacity (Rafatullah et al. 2009; Rahman and Islam 2009; Marković et al. 2011; Bernard and Jimoh 2013).

WCPO-based CNTs also demonstrate superior adsorption capacity compared with the chemically functionalized and acid-treated MWCNTs, such as amine-functionalized Fe_3O_4 nanoparticles (MNP–NH_2) (Hao et al. 2010) and nitric–sulfuric acid (*t*-MWCNTs) (Wang et al. 2013), respectively. MNP–NH_2 and *t*-MWCNTs appeared in the range of 5–74% and 15–94% of Cu (II) removal by using 0.01–1.0 and 0.1–1.0 g adsorbent dosage at low initial concentrations of 10 and 12 mg/L, respectively (Hao et al. 2010; Wang et al. 2013). Apart of excellent heavy metal adsorption capacity of heavy metal ions, WCPO-based CNTs also offer easy and environmental friendly preparation set-up and inexpensive absorbent compared with chemically functionalized (MNP–NH_2) and acid-treated MWCNTs (*t*-MWCNTs) because the preparation of chemically functionalized and acid-treated MWCNTs involved complex procedures, time consumption, and the use of hazardous chemical for these treatments (Ali et al. 2016). The comparison of Cu (II) adsorption by using different adsorbent materials is tabulated in Table 1.

Effect of initial pH solution

The effect of initial pH on Cu (II) adsorption capacity in the solution was studied in the range of 1–7 by using 1.8 g WCPO-based CNTs as an adsorbent with an initial concentration of 100 mg/L. The relationship between the initial pH solution values and the removal percentage of Cu (II) by WCPO-based CNTs is presented in Fig. 3. In general, the percentage of Cu (II) removal increases as the initial pH increases from 1 to 6 and achieves its saturation level at pH 7. In this study, at a low initial pH solution range from 1 to 3 (strongly acidic medium), a minimum removal percentage of Cu (II) in the range of ~76–81% is believed to be due to high H^+ ions generated by the protonation of electron on the adsorbent surface, and the predominant Cu (II) species in the solution was Cu^{2+} (Lu et al. 2006). Thus, the competition between H^+ and Cu^{2+} on the same sites of WCPO-based CNT surface hinders Cu^{2+} from approaching the active sites (Rafatullah et al. 2009). The increases in initial pH from 3 to 6 also yield in the increased percentage of removal for Cu (II) from ~81 to 99% before the equilibrium state is reached at an initial pH of 7. The possible explanation for higher Cu (II) removal was believed to be due to the increase in deprotonation, which enhances the electrostatic attraction forces between the surface of WCPO-based CNTs and heavy metal ions (Rao et al. 2007).

These findings were similar to those reported in the literature for the adsorption of Cu (II) by using fossil fuel-based MWCNTs synthesized by Pyrzyńska et al. (Pyrzyńska and Bystrzejewski 2010) and Wang et al. (Wang et al. 2013). At the initial pH range of 2 to 7 by using 0.05 to 0.5 g MWCNT

Table 1 Type of adsorbent materials used for Cu (II) removal

Adsorbent materials	Removal percentage of Cu (II) (%)	Adsorbent dosage (g/L)	Initial concentration of Cu (II) (mg/L)	Initial pH	Maximum adsorption capacity of Cu (II), q_m (mg/g)	Model	Reference
CNTs from acetylene	50–95	0.05–0.10	10	5.5	99	Freundlich	(Mubarak et al. 2015)
Functionalized MWCNTs	The highest; 93	0.001–0.01	20	3	118.41	Langmuir	(Gupta et al. 2017)
Activated carbon from banana peel	The tested value; 40.4	0.8–9.2	85	6.5	14.3	Langmuir	(Van Thuan et al. 2017)
Sesame seed cake	45–99	0.25–1	10	5	4.24	Langmuir	(Kumar et al. 2019)
Magnetic tubular carbon nanofibers	35–99.9	0.05–0.5	50	6	375.93	Langmuir	(Ahmad et al. 2020)
Iron oxide magnetic nanoparticles	The highest; 92	0.0025–0.04	0.048	9	0.7	Freundlich	(Almomani et al. 2020)
Potassium permanganate-modified pineapple cellulose	The highest; 95.5	5-20	1000	7	2.39	Freundlich and pseudo-second order	(Zhuang et al. 2020)
CNTs from WCPO	65–99 28–99	0.05–0.10 0.2–2.2	10 100	7	31.25	Langmuir	This work

adsorbent with low initial concentration of 10–12 mg/L, Pyrzyńska and Bystrzejewski (2010) and Wang et al. (2013) successfully removed ~5–65% and ~ 20–96% of Cu (II) from the solution, respectively. In comparison with our work, which used a solution with a low initial Cu (II) concentration solution of 10 mg/L, WCPO-based CNTs demonstrate excellent performance as an adsorbent material for Cu (II) removal compared with the previous study (Rao et al. 2009; Ma et al. 2012). Almost ~99% Cu (II) ions were successfully removed from the solution by using a small amount of CNTs of 0.1 g at pH of 7. The experiment cannot be continued at pH solution exceeding 7 because the precipitation of copper hydroxides ($Cu(OH)_2$) can occur as low as pH of 7.1 (Kamari and Ngah 2010). $Cu(OH)_2$ precipitation usually occurs in a solution at as early as 10 h prior to complete precipitation within 100 h (Karami 2013). Hence, the initial pH of 7 was considered as the optimum pH to remove ~99% of Cu (II) for both lower and higher initial Cu concentration of 10 and 100 mg/L by 0.1 and 1.8 g WCPO-based CNT adsorbent, respectively. Table 1 shows the effect of pH for the adsorption of Cu (II) as obtained by the other study that used various adsorbent materials (Rafatullah et al. 2009; Rahman and Islam 2009; Hao et al. 2010; Marković et al. 2011; Kosa et al. 2012; Bernard and Jimoh 2013; Wang et al. 2013; Mubarak et al. 2015).

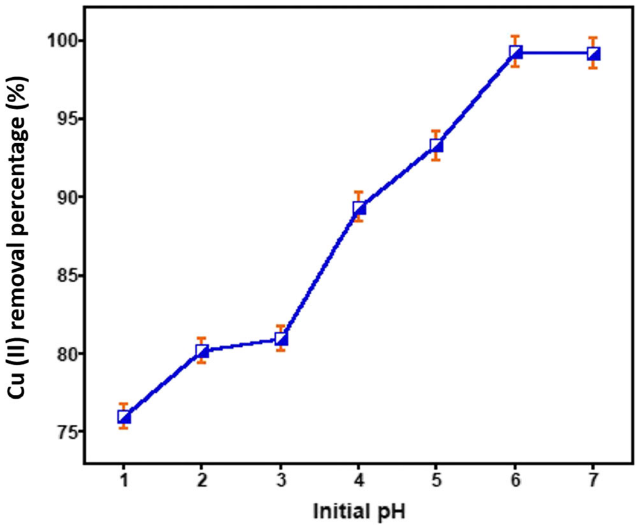

Fig. 3 Effect of pH solution (1–7) on the adsorption of Cu (II) by using 1.8 g WCPO-based CNT adsorbent with 100 mg/L initial concentration

Effect of different heavy metal ions

Contaminated water typically contains more than one heavy metal, such as Cu, Fe, Zn, and others. Therefore, the study of adsorption of heavy metal ions by using a variety of metal ions, such as Zn (II) and Fe (II), has been extended. The experiments were carried out using Zn (II) and Fe (II) at initial concentration solution of 100 mg/L and pH solution of 7 by using 0.6–1.8 g WCPO-based CNT adsorbent. The same adsorption trend was observed, similar to the adsorption of Cu (II) as previously explained. The adsorption capacity of all three metal ions improves with the increase in CNT dosage from 0.6 to 1.8 g. Figure 4a shows the removal percentage of metal ions by using WCPO-based CNT adsorbent in the range

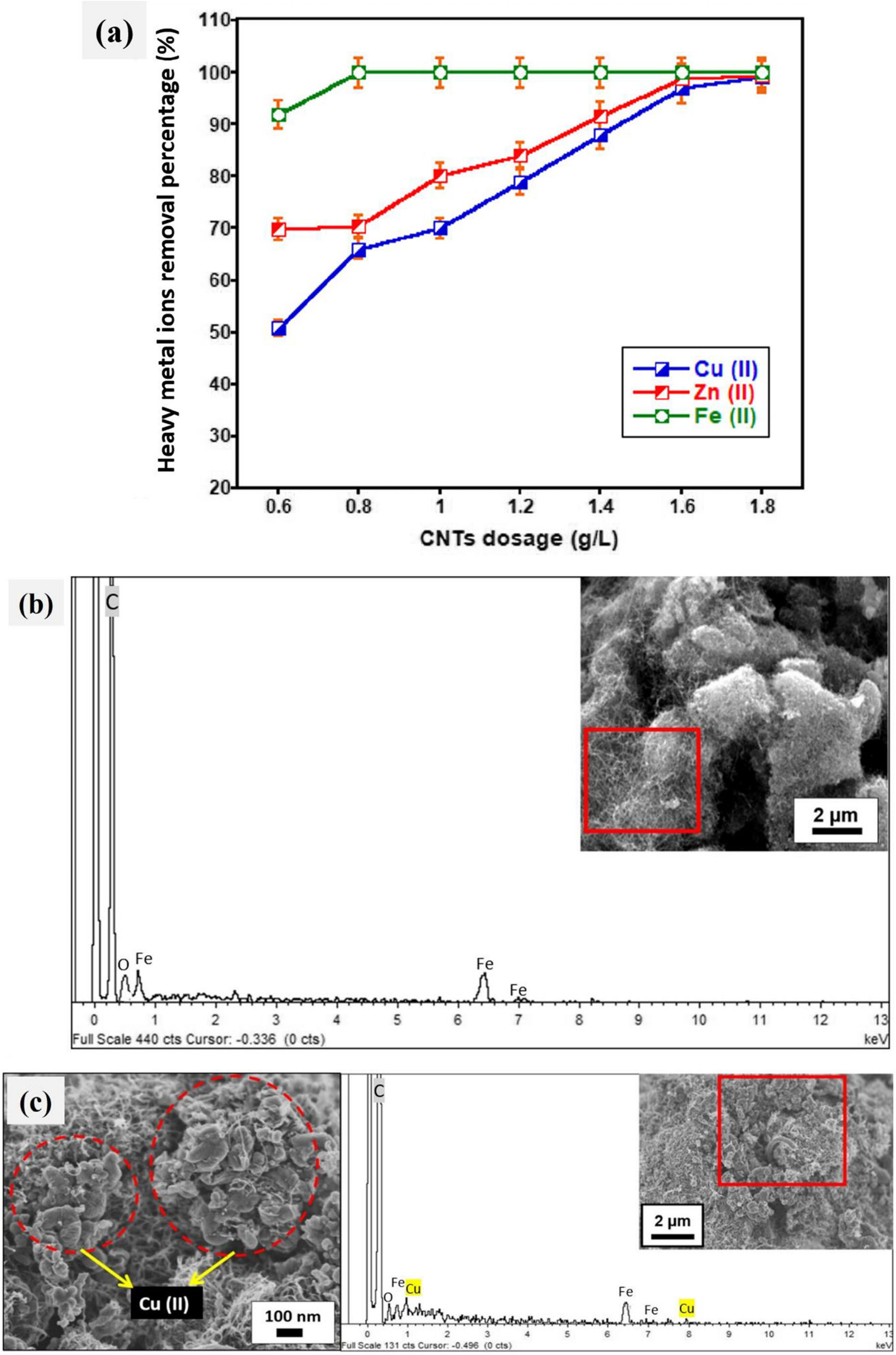
(a)
Heavy metal ions removal percentage (%)
110
100
90
80
70
60
50
40
30
20
0.6
0.8
1
1.2
1.4
1.6
1.8
CNTs dosage (g/L)
Cu (II)
Zn (II)
Fe (II)
(b)
C
O
Fe
Fe
Fe
0
1
2
3
4
5
6
7
8
9
10
11
12
13
Full Scale 440 cts Cursor: -0.336 (0 cts)
keV
2 µm
(c)
Cu (II)
100 nm
C
O
Fe
Cu
Fe
Fe
Cu
Full Scale 131 cts Cursor: -0.496 (0 cts)
keV
2 µm

◀ **Fig. 4** **a** Removal percentage of Cu (II), Zn (II), and Fe (II) by using 0.6–1.8 g WCPO-based CNT adsorbent. FESEM and EDS analysis **b** before and **c**–**e** after the adsorption of Cu (II), Zn (II), and Fe (II), respectively, by using 1.8 g WCPO-based CNT adsorbent with 100 mg/L initial concentration and at pH of 7. **f** FTIR spectra of WCPO-based CNTs before and after adsorption of Cu (II), Zn (II), and Fe (II)

of 91.9–99.9%, 69.9–99.5%, and 50.8–99.2% for Fe (II), Zn (II), and Cu (II), respectively. Interestingly, Fe (II) was substantially removed (99.9%) by only 0.8 g WCPO-based CNT adsorbent prior to achieving the saturation level (see Fig. 4) compared with Zn (II) and Cu (II), which require higher amounts of CNT-based WCPO (1.8 g) for substantial removal of the ions from the solution (~99%). With as low as 0.6 g CNT adsorbent, the removal percentage of Zn (II) was observed at ~69.9% as compared with Cu (II) removal of ~50.8%. The comparison between Zn (II) and Cu (II) adsorption capacity in this study is consistent with the study by Kosa et al. (Kosa et al. 2012), in which 0.05 g MWCNT adsorbent removed approximately ~72% and 70% of Zn (II) and Cu (II), respectively, from the solution with low initial concentration and pH of 1 mg/L and 5, respectively. Hence, the adsorption capacity of WCPO-based CNTs for different metal ions in this study was in the following order: Fe (II) > Zn (II) ≈ Cu (II). This order is also consistent with the report by Karami et al. (Karami 2013), in which about ~75%, 60%, and 50% of Fe (II), Zn (II), and Cu (II), respectively, (Fe (II) > Zn (II) > Cu (II)) were removed by using 0.50 g magnetite nanorod adsorbent at pH of 5.5 with high initial solution concentration. The decrease in the ionic radius of metal ions from 0.61 to 0.74 Å is shown in the following order: Fe 0.61 Å > Cu 0.73 Å ≈Zn (0.74) Å. The trend shows higher adsorption on the CNT surface compared with larger ionic radius (Arshadi et al. 2014; Franus and Bandura 2014). This finding was believed to be due to better penetration of metal ions via the boundary layer of CNT absorbent, subsequently followed by easier adsorption on the CNT surface by smaller ionic radius (Kosa et al. 2012).

Figure 4b–e shows the EDS analysis of WCPO-based CNTs before the adsorption of Fe (II), Zn (II), and Cu (II). The trace of carbon (92.18%), oxygen (2.97%), and iron (4.85%) elements was the major constituents in the adsorbent material. After the adsorption of Fe (II), Zn (II), and Cu (II), significant changes were observed on the surface morphology of WCPO-based CNT adsorbent and were supported by FESEM and EDS analysis. The appearance of flake- and lump-like deposits on CNT surface was observed after adsorption process. In general, after adsorption, functional groups, such as hydroxyl, carboxyl, and carbonyl groups, are formed through adsorption and attached to the surface of WCPO-based CNTs or any active defect site (Das et al. 2014; Mubarak et al. 2016). Therefore, after the adsorption of heavy metal ions, the surface of WCPO-based CNTs was less smooth than that before adsorption. After the adsorption of metal ions, the presence of Fe (II), Zn (II), and Cu (II) peak was confirmed by EDS analysis. Thus, WCPO-based CNTs exhibit excellent performance in the adsorption of Fe (II), Zn (II), and Cu (II) from the solution. Meanwhile, the presence of Fe in all samples was due to the ferrocene catalyst consumed during the synthesis of WCPO-based CNTs.

In this study, better adsorption of metal ions, namely, Fe (II), Zn (II), and Cu (II), depends on the functional groups in the adsorbent material. Figure 4f shows the FTIR spectrum before and after adsorption of metal ions on the surface of CNTs from WCPO. Peaks observed before adsorption of metal ions were detected at 1287 and 1600 cm^{-1}, which are defined as C-O stretching and aromatic C=C groups, followed by the carbonyl (C=O) and hydroxyl groups (O-H) at 1740 and 2700 cm^{-1}, respectively (Li et al. 2003; Kamari et al. 2014; Yusoff et al. 2014; Mubarak et al. 2016). Meanwhile, a broad peak in the range of 3250–3550 cm^{-1} was assigned as O-H stretching from carboxyl groups (O=C-OH and C-OH) (Mubarak et al. 2015; Vázquez et al. 2016). Carboxyl, carbonyl, and hydroxyl groups are known as acidic functional groups that exist on the CNT surface owing to oxidation during post-annealing treatment at 500 °C under ambient oxygen (Edwards et al. 2011). The presence of the functional groups on the adsorbent surface may enhance cation exchange site and produce electrostatic interaction, thus leading to better adsorption capacity of metal ions on the adsorbent surface (Tofighy and Mohammadi 2011). After metal ion adsorption, new peaks appeared in the range of 784–809 and 996–998 cm^{-1}, indicating the characteristics of (Fe, Zn, Cu) = O and (Fe, Zn, Cu)-O stretching frequencies, respectively (Rahman and Islam 2009). Adsorption between CNTs from WCPO and metal ions was proven with the disappearance of the carbonyl and hydroxyl peaks at 1740 and 2700 cm^{-1} after adsorption (Vázquez et al. 2016). The shifts in the amine peak from 1600 cm to 1620–1626 cm^{-1} and carbonyl groups from 1287 to 1302–1315 cm^{-1}, respectively, were believed to be due to the interaction between the heavy metal ions with the active site of WCPO-based CNTs through chemical complexion and electrostatic interaction (Sun et al. 2014; Yusoff et al. 2014; Mubarak et al. 2016).

Adsorption isotherm model

To understand the adsorption of Cu (II) on the WCPO-based CNT absorbent, Langmuir and Freundlich isotherm models were then used to explain the behavior of metal ion at equilibrium between adsorbed Cu (II) on CNTs at different dosages of 0.2–2.2 g with 100 mg/L initial concentration of Cu (II) solution at pH of 7. The linear form of Langmuir model can be represented as the following equations (Foo and Hameed 2010; Adeli et al. 2017; Palanivell et al. 2020):

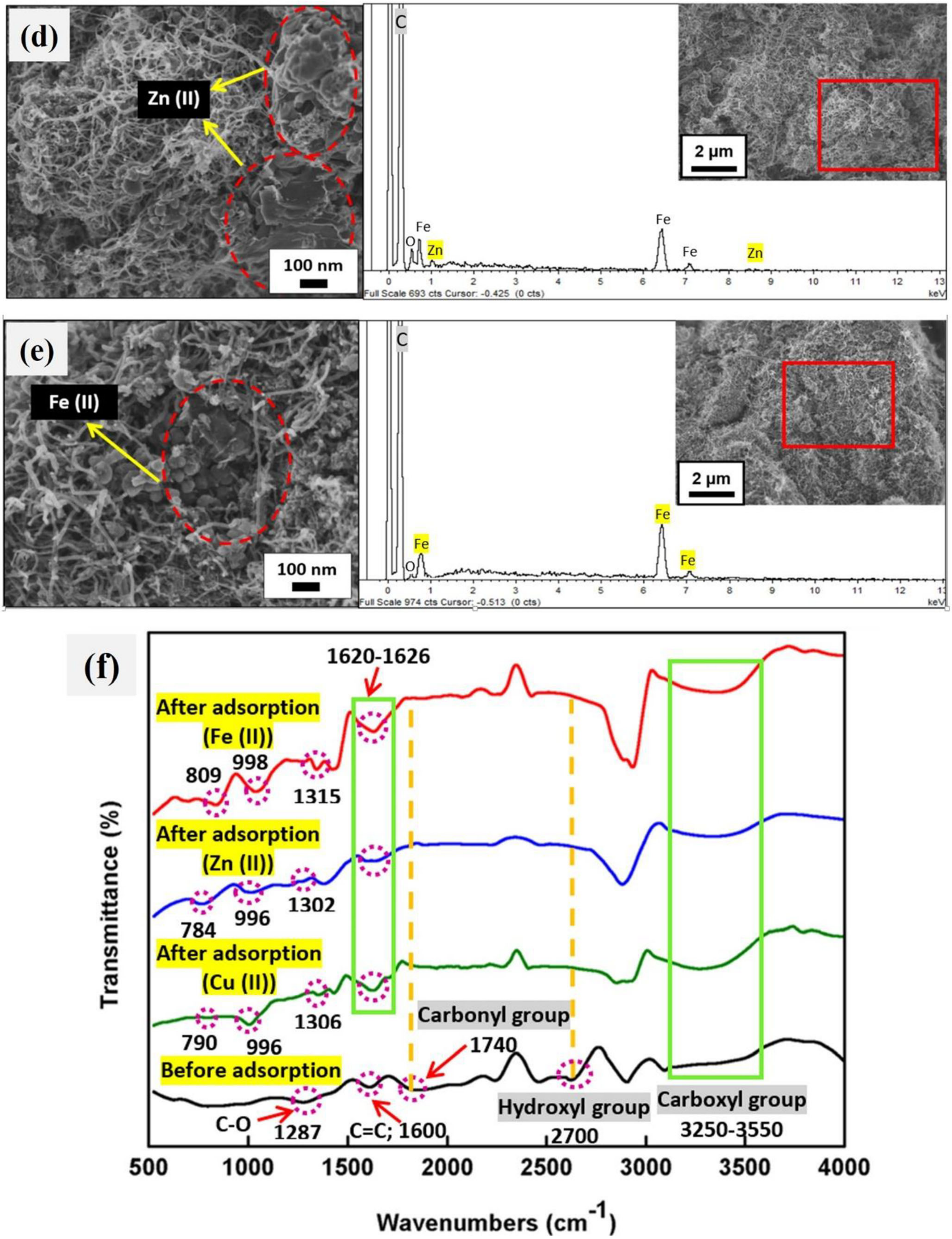

Fig. 4 (continued)

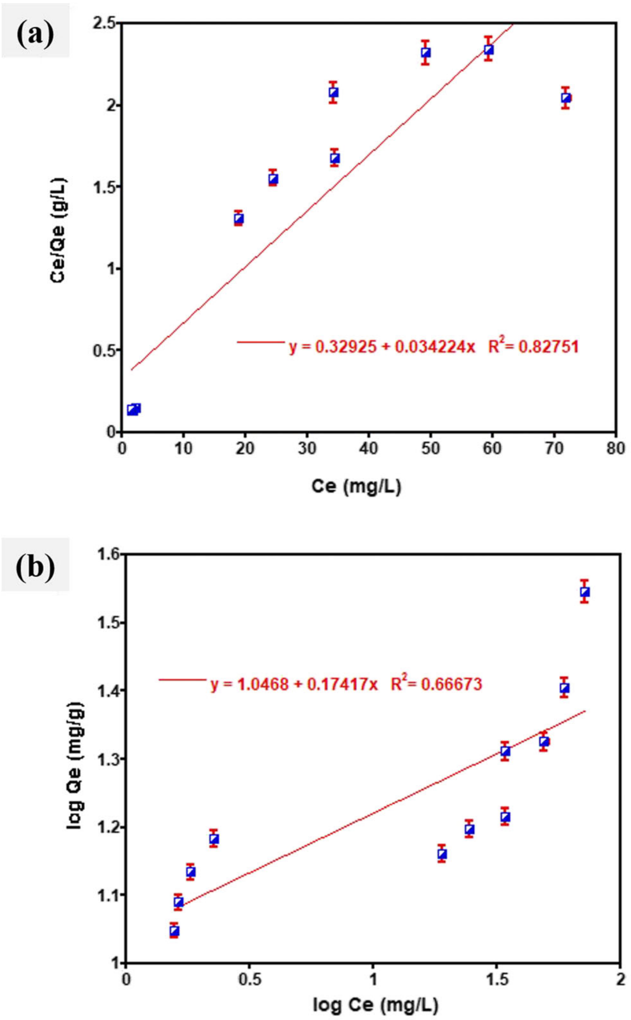

Fig. 5 **a** Langmuir and **b** Freundlich isotherm models for the adsorption of Cu (II) by using 0.2–2.2 g WCPO-based CNT adsorbent at the initial concentration and pH of 100 mg/L and 7, respectively

$$\frac{C_e}{q_e} = \frac{1}{K_L q_m} + \frac{C_e}{q_m} \tag{3}$$

where q_e (mg/g) represents equilibrium adsorption capacity, C_e (mg/L) is the equilibrium heavy metal ion concentration (mg/L), q_m (mg/g) is the maximum adsorption capacity of the metal ions (mg/g), and K_L is the Langmuir adsorption constant (L/mg), which is related to the free energy of heavy metal ion adsorption. The graph of C_e/q_e versus C_e presented in Fig. 5a was plotted and fitted with linear equation of $y = 0.034224\,x + 0.32925$, where the slope^{-1} and slope/intercept represent q_m and K_L, respectively (Palanivell et al. 2020). Based on calculation, $q_m$and K_L were found to be 29.22 mg/g and 0.1039 L/mg, respectively. A correlation coefficient (R^2) of 0.82751 was obtained for Cu (II) adsorption with this model, indicating that the experimental data were in good accordance with Langmuir model. The Langmuir model assumes that the adsorption of heavy metal ions occurs and forms monolayers on the surface or active sites of the adsorbent (Kumar et al. 2019). The essential characteristic of the Langmuir model also could be described by the equilibrium constant, R_L, which is defined as follows (Foo and Hameed 2010; Adeli et al. 2017):

$$R_L = \frac{1}{1 + K_L C_o} \tag{4}$$

an R_L value of 0.0878 was obtained in this study, indicating favorable adsorption of Cu (II) by the WCPO-based CNT adsorbent (Foo and Hameed 2010).

Meanwhile, the Freundlich isotherm model deals with the adsorption of heavy metal ions on a multilayer heterogeneous surface of adsorbent. The linear form of Freundlich isotherm equation is given as follows (Foo and Hameed 2010; Ma et al. 2015; Palanivell et al. 2020):

$$\log q_e = \frac{1}{n}\log C_e + \log K_F \tag{5}$$

where K_F (mg/g (L/mg)$^{1/n}$) and $1/n$ are Freundlich isotherm constants and heterogeneity factor, respectively (Alves et al. 2019). Figure 5b shows the linear Freundlich isotherm plot fitted with the equation of $y = 0.17417x + 1.0468$, where the antilog (intercept) and slope represent K_F (11.1378) and $1/n$ (0.1742), respectively (Palanivell et al. 2020). According to the Freundlich model, adsorption was favorable when $1/n$ is between 0 and 1, and lower $1/n$ value indicates that the adsorbent possesses more heterogeneous binding sites (Ahmadpour et al. 2014). The R^2 for Freundlich model is 0.66673, which is lower than that of the Langmuir model (0.82751). Hence, a high validity of the Langmuir model is proposed, in which during adsorption, Cu (II) ions form a monolayer coverage on the CNT surface, and the uniform adsorption energies are equal for all adsorption sites (Adeli et al. 2017; Palanivell et al. 2020). Similar findings also followed the Langmuir model, as observed by Gupta et al. when utilizing functionalized MWCNTs for fact adsorption of Cu (II); Langmuir and Freundlich R^2 values were 0.9998 and 0.9821, respectively

Table 2 Parameters of Langmuir and Freundlich isotherms for adsorption of Cu (II) using WCPO-based CNT adsorbent material at 0.2–2.2 g adsorbent dosage

Langmuir			Freundlich		
q_m (mg/g)	K_L (L/mg)	R^2	$1/n$	K_F (mg/g (L/mg)$^{1/n}$)	R^2
29.22	0.1039	0.82751	0.1742	11.1378	0.66673

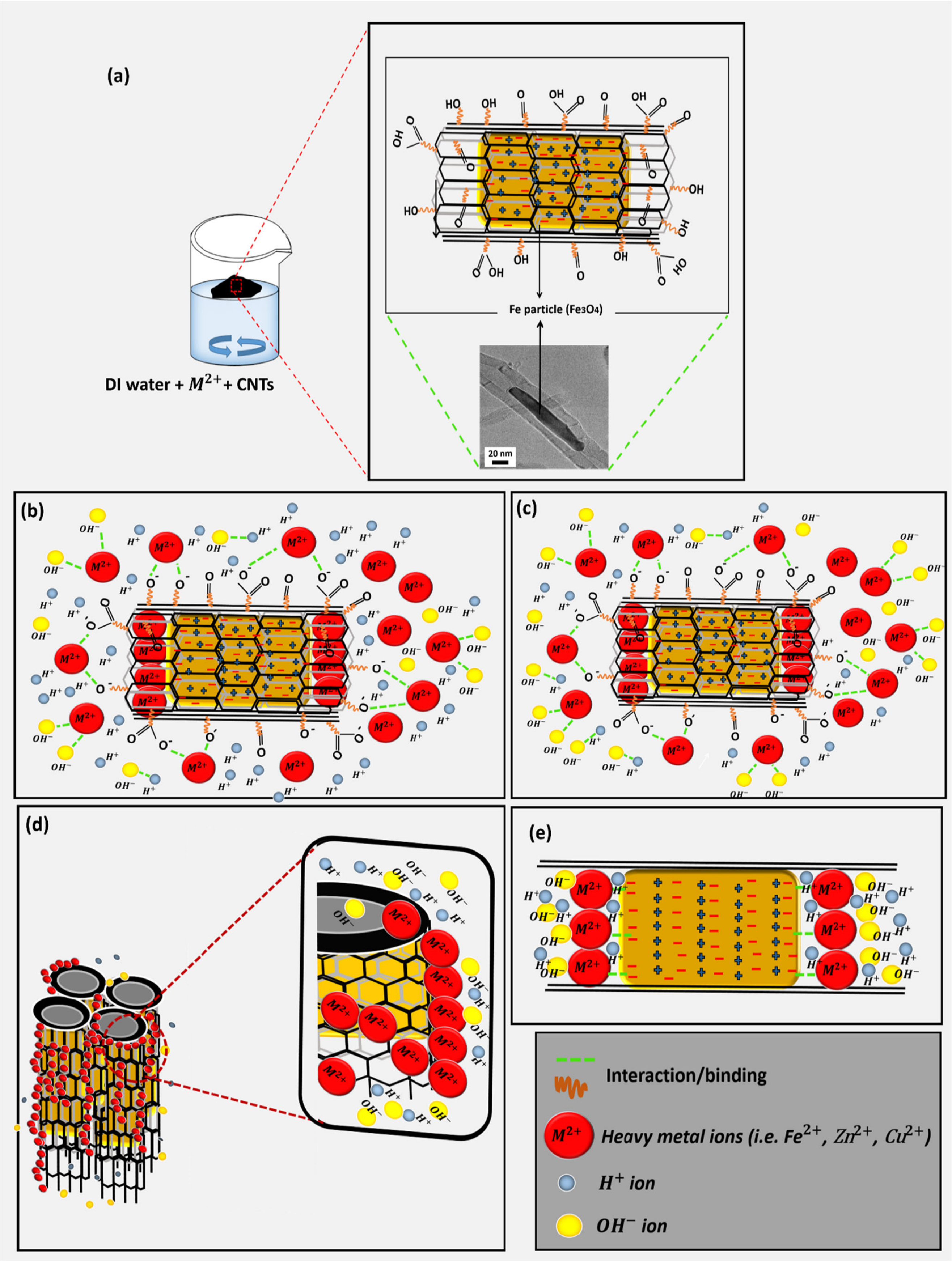
(a)
DI water + M^{2+} + CNTs
Fe particle (Fe3O4)
20 nm
(b)
(c)
(d)
(e)
Interaction/binding
M^{2+} Heavy metal ions (i.e. Fe^{2+}, Zn^{2+}, Cu^{2+})
H^+ ion
OH^- ion

◀ **Fig. 6** **a** The proposed adsorption mechanism of M (II) onto WCPO-based CNT adsorbent in **b** acidic medium (pH ranges 1–3); **c** at the pH range of 4–6; **d** adsorption metal ions on the CNT surface, defect sites, and **e** the inner tube of CNTs in the presence of Fe nanoparticles

(Gupta et al. 2017). The Langmuir and Freundlich models are summarized in Table 2.

Adsorption mechanism

The schematic diagram as in Fig. 6a–e illustrated the proposed adsorption mechanism of heavy metal ions, M^{2+} (where M represents the heavy metal ions), by using WCPO-based CNTs as adsorbent. The adsorption mechanisms were believed to include the electrostatic attraction and repulsion, chemical interaction between metal ions and the functional groups of carboxyl and hydroxyl groups of WCPO-based CNTs (Fig. 6a), adsorption precipitation, and chemical interaction with the defect sites in the adsorbent (Vuković et al. 2010). In addition, the presence of ferromagnetic behavior of CNTs was believed to participate during the metal ion adsorption.

Given that the uptake capacity of heavy metal ions is dominated by the pH solution, the adsorption mechanism was carried out by systematically investigating the effect of solution pH toward the adsorption of heavy metal ions by WCPO-based CNTs. In highly acidic medium as shown in Fig. 6b, heavy metal ions were predominantly M^{2+} ions (Sočo and Kalembkiewicz 2015). Equations (6) and (7) show the suggested reaction for the protonation of electron on carboxyl and hydroxyl groups on the surface of WCPO-based CNTs that resulted in positively charged (H^+) dominating in the solution. The competition between H^+ from the acidic medium and M^{2+} on the active sites of the CNT adsorbent (CNT–COO$^-$ and CNT–CO$^-$) generates the electrostatic repulsion force, which decreases the adsorption of metal ions in the solution.

$$M^{2+} + 2(\mathrm{CNTs{-}COOH}) + H_2O + H^+ \rightarrow (\mathrm{CNTs{-}COO})_2M + 3H^+ + OH^- \quad (6)$$

$$M^{2+} + 2(\mathrm{CNTs{-}COH}) + H_2O + H^+ \rightarrow (\mathrm{CNTs{-}CO})_2M + 3H^+ + OH^- \quad (7)$$

By increasing pH solution from 4 to 7 (Fig. 6c), the CNT surface charge changed to negative charge, and the competition between M^{2+} and H^+ was decreased at higher pH solution. Thus, more M^{2+} took place on the negative surface sites of the CNTs, which was due to the deprotonation of electron on the functional group of WCPO-based CNTs (carboxyl and hydroxyl groups) and produced higher electrostatic attraction force between the surface of WCPO-based CNTs and metal ions. Therefore, the difference in uptake capacity of metal ion absorption at variation of pH was also attributed by the carboxyl and hydroxyl groups on the adsorbent surface where the functional group induced negative charge on the WCPO-based CNTs and led to exchangeability of proton in the functional group with the metal ions.

In this study, the ionic radii of metal ions ranged between 0.061 and 0.074 nm, which is significantly smaller than the interlayer spacing of WCPO-based CNT adsorbent, which is 0.33 nm; thus, the surface adsorption of metal ions was also believed to occur on the internal and external wall surfaces of CNTs. The proposed surface adsorption mechanism on the external surface of CNTs also adhered with the Langmuir model isotherm, which proposes that the adsorbed metal ions form a monolayer coverage on the CNT surface, as illustrated in Fig. 6d (Bayazit and Kerkez 2014). When WCPO-based CNT powdered solid adsorbents were made in contact with the metal ions in the solution, the metal ions migrate first from the bulk solution to the surface of the CNT absorbent before they impose a diffusion barrier (Gupta et al. 2005). The uptake capacity of metal ions by the WCPO-based CNTs is controlled by internal and external diffusion of the adsorbent (Gupta et al. 2005; Mahalingam et al. 2013). Four possibilities of adsorption mechanism were believed to occur during the adsorption of metal ions onto the WCPO-based CNT adsorbent, as is in agreement with the four consecutive steps of adsorption proposed by Gupta and P. Mahalingam et al. (Gupta et al. 2005; Mahalingam et al. 2013). The adsorption of heavy metal ion on the WCPO-based CNTs is proposed as follows: (i) the external mass of heavy metal ions transport from the bulk solution to the WCPO-based CNT adsorbent particles; (ii) the heavy metal ions transport to the external CNT surface (external diffusion); (iii) the transport of heavy metal ions within the pores of the WCPO-based CNT pores except for a small amount of adsorption, which is believed to occur on the external surface known as internal or particle diffusion; and (iv) lastly, the adsorption of heavy metal ions onto the interior surface of WCPO-based CNTs (Gupta et al. 2005; Mahalingam et al. 2013). The proposed mechanism for the adsorption metal ions onto the CNT surface is divided into two parts; steps (i) and (ii) represent the external diffusion, whereas steps (iii) and (iv) represent the internal diffusion for metal ion adsorption. Hence, Eq. (8) has been proposed to represent the suggested mechanism of the adsorption phenomenon, proving that the external and internal surfaces of adsorbent were involved for the adsorption of metal ions in solution.

$$M^{2+} + C_xH_y + H_2O \rightarrow M(C_xH_y)_2 + 2H^+ + OH^- \quad (8)$$

The adsorption mechanism also depended on the defect sites of WCPO-based CNT adsorbent that can be exhibited to be capable at relatively high surface reactivity and promotes radical sites of CNT structure (C$^-$), subsequently forming dangling bonds (Machado et al. 2015). This finding offers an advantage for metal ions in the solution to attach onto dangling bond spaces of the adsorbent, as shown in Eq. (9). The highly reactive sites of WCPO-based CNTs increased the number of metal ions onto the adsorbent surfaces and thus increases the adsorption of metal ions.

$$M^{2+} + 2C^{-} + H_2O + H^{+} \rightarrow MC_2 + 2H^{+} + OH^{-} \qquad (9)$$

where $x, y \geq 1$.

The presence of Fe nanoparticles in the inner tube of CNTs offers advantages as adsorbent material; Fe nanoparticles (also known as Fe_3O_4) are believed to act as a magnet (Miyamoto et al. 2005). The Fe nanoparticles were believed to possess temporary dipole moment, and the WCPO-based CNT surface charge can turn into a negative charge. Thus, the interaction between Fe nanoparticles and heavy metal ions will occur at the inner tube of CNTs, as illustrated in Fig. 6e (Miyamoto et al. 2005; Khandanlou et al. 2015). Meanwhile, at higher pH value, which is considerably higher than 7 (pH > 8), the precipitation of metal ions occurs in their hydroxide form ($M(OH)_2$) (Pyrzyńska and Bystrzejewski 2010; Yusoff et al. 2014).

Conclusion

WCPO-based CNTs encapsulated Fe nanoparticle have been successfully produced through modified thermal chemical vapor deposition and applied as adsorbent of heavy metal ions. Based on the first parameter measurement, higher Cu (II) ion removal percentage was achieved by increasing adsorbent dosage from 0.6 to 1.8 g/L then saturated from 1.8 to 2.2 g/L. Therefore, 1.8 g/L was chosen as the optimum adsorbent dosage with the highest Cu (II) ion removal percentage of ~99% at neutral solution (pH 7). Second parameter measurement showed that high Cu (II) ion removal percentage (~80%) was also achieved even in a very acidic solution (pH 2). The last parameter measurement also showed that the produced WCPO-based CNTs successfully removed various heavy metal ion removal in the range of 99.2 to 99.9% with the order of Fe (II) > Zn (II) ≈ Cu (II). The adsorption mechanism involves the chemical reaction between the functional groups of adsorbents and metal ions, electrostatic interaction (attraction and repulsion force), adsorbent surface defects, and the presence of Fe nanoparticles, which act as magnets to interact with metal ions during adsorption. In addition, the adsorption behaviors of metal ions by using WCPO–based CNTs match well with the Langmuir isotherm model, yielding a higher correlation coefficient and maximum adsorption capacity metal ions of 0.82751 and 29.22 mg/g, respectively. Moreover, the encapsulated Fe particles act as magnets to interact with metal ions during adsorption. This findings showed that the produced WCPO-based CNTs can be a promising material to be applied as adsorbent for heavy metal ions removal for large-volume applications.

Materials availability The datasets generated and/or analyzed during the current study are not publicly available due to technical or time limitations.

Author contribution All authors contributed to the study conception and design as stated below:

- Conceptualization and supervision: Suriani Abu Bakar
- Methodology: Suriani Abu Bakar and Norhafizah Jusoh
- Formal analysis and investigation: Norhafizah Jusoh
- Writing (original draft preparation): Norhafizah Jusoh
- Writing (review and editing): Suriani Abu Bakar, Azmi Mohamed, Muqoyyanah Muqoyyanah, Mohd Hafiz Dzarfan Othman, Mohamad Hafiz Mamat, Mohd Khairul Ahmad, Mohd Ambri Mohamed, Muhammad Noor Azlan, Norhayati Hashim, Muhammad Danang Birowosuto, and Tetsuo Soga.

Prior to the submission, all authors have read and approved the final manuscript.

Funding The authors acknowledge the financial support from the PRGS (grant no. 2013-0097-102-32) grants and UPSI.

Data availability The datasets generated and/or analyzed during the current study are not publicly available due to legal or ethical reasons. The datasets generated and/or analysed during the current study are not publicly available due to technical or time limitations.

Declarations

Ethics approval and consent to participate Not applicable.

Consent for publication Not applicable.

Competing interests The authors declare no competing interests.

References

Adeli M, Yamini Y, Faraji M (2017) Removal of copper, nickel and zinc by sodium dodecyl sulphate coated magnetite nanoparticles from water and wastewater samples. Arab J Chem 10:S514–S521. https://doi.org/10.1016/j.arabjc.2012.10.012

Ahangari A, Raygan S, Ataie A (2019) Capabilities of nickel zinc ferrite and its nanocomposite with CNT for adsorption of arsenic (V) ions from wastewater. J Environ Chem Eng 7:103493. https://doi.org/10.1016/j.jece.2019.103493

Ahmad A, Rafatullah M, Sulaiman O, Ibrahim MH, Chii YY, Siddique BM (2009) Removal of Cu(II) and Pb(II) ions from aqueous solutions by adsorption on sawdust of Meranti wood. Desalination 247:636–646. https://doi.org/10.1016/j.desal.2009.01.007

Ahmad M, Wang J, Xu J, Zhang Q, Zhang B (2020) Magnetic tubular carbon nanofibers as efficient Cu (II) ion adsorbent from wastewater. J Clean Prod 252:119825. https://doi.org/10.1016/j.jclepro.2019.119825

Ahmadpour A, Eftekhari N, Ayati A (2014) Performance of MWCNTs and a low-cost adsorbent for chromium(VI) ion removal. J

Nanostruct Chem 4:171–178. https://doi.org/10.1007/s40097-014-0119-9

Ali WNNW, Sufian S, Abdullah MZ (2016) Green functionalization: comparison of different carbonaceous materials. Procedia Eng 148:795–805. https://doi.org/10.1016/j.proeng.2016.06.566

Almomani F, Bhosale R, Khraisheh M, kumar A, Almomani T (2020) Heavy metal ions removal from industrial wastewater using magnetic nanoparticles (MNP). Appl Surf Sci 506:144924. https://doi.org/10.1016/j.apsusc.2019.144924

Alves DCS, Goncalves JO, Coseglio BB et al (2019) Adsorption of phenol onto chitosan hydrogel scaffold modified with carbon nanotubes. J Environ Chem Eng 7:103460. https://doi.org/10.1016/j.jece.2019.103460

Amen R, Yaseen M, Mukhtar A, Klemeš JJ, Saqib S, Ullah S, al-Sehemi AG, Rafiq S, Babar M, Fatt CL, Ibrahim M, Asif S, Qureshi KS, Akbar MM, Bokhari A (2020) Lead and cadmium removal from wastewater using eco-friendly biochar adsorbent derived from rice husk, wheat straw, and corncob. Clean Eng Technol 1:100006. https://doi.org/10.1016/j.clet.2020.100006

Arshadi M, Amiri M J, Mousavi S (2014) Kinetic, equilibrium and thermodynamic investigations of Ni (II), Cd (II), Cu (II) and Co (II) adsorption on barley straw ash Water Resources and Industry 6:1–17 https://doi.org/10.1016/j.wri.2014.06.001

Balintova M, Holub M, Singovszka E (2012) Study of iron, copper and zinc removal from acidic solutions by sorption. Chem Eng Trans 28: 175–180. https://doi.org/10.3303/CET1228030

Bartczak P, Norman M, Klapiszewski Ł, Karwańska N, Kawalec M, Baczyńska M, Wysokowski M, Zdarta J, Ciesielczyk F, Jesionowski T (2018) Removal of nickel(II) and lead(II) ions from aqueous solution using peat as a low-cost adsorbent: a kinetic and equilibrium study. Arab J Chem 11:1209–1222. https://doi.org/10.1016/j.arabjc.2015.07.018

Bayazit ŞS, Kerkez Ö (2014) Hexavalent chromium adsorption on superparamagnetic multi-wall carbon nanotubes and activated carbon composites. Chem Eng Res Des 92:2725–2733. https://doi.org/10.1016/j.cherd.2014.02.007

Bernard E, Jimoh A (2013) Adsorption of Pb, Fe, Cu, and Zn from industrial electroplating wastewater by orange peel. Int J Eng Appl Sci 4:95–103

Bollen P, Quievy N, Detrembleur C, Thomassin JM, Monnereau L, Bailly C, Huynen I, Pardoen T (2016) Processing of a new class of multifunctional hybrid for electromagnetic absorption based on a foam filled honeycomb. Mater Des 89:323–334. https://doi.org/10.1016/j.matdes.2015.09.129

Božić D, Stanković V, Gorgievski M, Bogdanović G, Kovačević R (2009) Adsorption of heavy metal ions by sawdust of deciduous trees. J Hazard Mater 171:684–692. https://doi.org/10.1016/j.jhazmat.2009.06.055

Briffa J, Sinagra E, Blundell R (2020) Heavy metal pollution in the environment and their toxicological effects on humans. Heliyon 6: e04691. https://doi.org/10.1016/j.heliyon.2020.e04691

Chwastowski J, Staroń P, Kołoczek H, Banach M (2017) Adsorption of hexavalent chromium from aqueous solutions using Canadian peat and coconut fiber. J Mol Liq 248:981–989. https://doi.org/10.1016/j.molliq.2017.10.152

Das R, Abd Hamid SB, Ali ME, Ismail AF, Annuar MSM, Ramakrishna S (2014) Multifunctional carbon nanotubes in water treatment: the present, past and future. Desalination 354:160–179. https://doi.org/10.1016/j.desal.2014.09.032

Duan C, Ma T, Wang J, Zhou Y (2020) Removal of heavy metals from aqueous solution using carbon-based adsorbents: a review. J Water Process Eng 37:101339. https://doi.org/10.1016/j.jwpe.2020.101339

Edwards ER, Antunes EF, Botelho EC, Baldan MR, Corat EJ (2011) Evaluation of residual iron in carbon nanotubes purified by acid treatments. Appl Surf Sci 258:641–648. https://doi.org/10.1016/j.apsusc.2011.07.032

Fernández-Luqueño F, López-Valdez F, Gamero-Melo P et al (2013) Heavy metal pollution in drinking water - a global risk for human health: a review. Afr J Environ Sci Technol 7:567–584. https://doi.org/10.5897/AJEST12.197

Foo KY, Hameed BH (2010) Insights into the modeling of adsorption isotherm systems. Chem Eng J 156:2–10. https://doi.org/10.1016/j.cej.2009.09.013

Franus M, Bandura L (2014) Sorption of heavy metal ions from aqueous solution by glauconite. Fresenius Environ Bull 23:825–839

Fu D, Ma Q, Zeng X, Chen J, Zhang W, Li D (2013) Synthesis and magnetic properties of aligned carbon nanotubes by microwave-assisted pyrolysis of acetylene. Phys E Low-Dim Syst Nanostruct 54:185–190. https://doi.org/10.1016/j.physe.2013.06.022

Gangupomu RH, Sattler ML, Ramirez D (2016) Comparative study of carbon nanotubes and granular activated carbon: physicochemical properties and adsorption capacities. J Hazard Mater 302:362–374. https://doi.org/10.1016/j.jhazmat.2015.09.002

Gao A, Xie K, Song X, Zhang K, Hou A (2017) Removal of the heavy metal ions from aqueous solution using modified natural biomaterial membrane based on silk fibroin. Ecol Eng 99:343–348. https://doi.org/10.1016/j.ecoleng.2016.11.008

Gupta VK, Mittal A, Gajbe V (2005) Adsorption and desorption studies of a water soluble dye, Quinoline Yellow, using waste materials. J Colloid Interface Sci 284:89–98. https://doi.org/10.1016/j.jcis.2004.09.055

Gupta VK, Agarwal S, Bharti AK, Sadegh H (2017) Adsorption mechanism of functionalized multi-walled carbon nanotubes for advanced Cu (II) removal. J Mol Liq 230:667–673. https://doi.org/10.1016/j.molliq.2017.01.083

Hao YM, Man C, Hu ZB (2010) Effective removal of Cu (II) ions from aqueous solution by amino-functionalized magnetic nanoparticles. J Hazard Mater 184:392–399. https://doi.org/10.1016/j.jhazmat.2010.08.048

Huang Z n, Wang X l, Yang D s (2015) Adsorption of Cr(VI) in wastewater using magnetic multi-wall carbon nanotubes. Water Sci Eng 8:226–232. https://doi.org/10.1016/j.wse.2015.01.009

Ihsanullah AA, Al-Amer AM et al (2016) Heavy metal removal from aqueous solution by advanced carbon nanotubes: critical review of adsorption applications. Sep Purif Technol 157:141–161. https://doi.org/10.1016/j.seppur.2015.11.039

Kamari A, Ngah WS (2010) Adsorption of Cu(II) and Cr(VI) onto treated shorea dasyphylla bark: isotherm, kinetics, and thermodynamic studies. Sep Sci Technol 45:486–496. https://doi.org/10.1080/01496390903526717

Kamari A, Yusoff SNM, Abdullah F, Putra WP (2014) Biosorptive removal of Cu(II), Ni(II) and Pb(II) ions from aqueous solutions using coconut dregs residue: adsorption and characterisation studies. J Environ Chem Eng 2:1912–1919. https://doi.org/10.1016/j.jece.2014.08.014

Karami H (2013) Heavy metal removal from water by magnetite nanorods. Chem Eng J 219:209–216. https://doi.org/10.1016/j.cej.2013.01.022

Khandanlou R, Ahmad MB, Masoumi HRF et al (2015) Rapid adsorption of copper(II) and lead(II) by rice straw/Fe_3O_4 nanocomposite: optimization, equilibrium isotherms, and adsorption kinetics study. PLoS One 10:1–19. https://doi.org/10.1371/journal.pone.0120264

Kosa SA, Al-Zhrani G, Abdel Salam M (2012) Removal of heavy metals from aqueous solutions by multi-walled carbon nanotubes modified with 8-hydroxyquinoline. Chem Eng J 181–182:159–168. https://doi.org/10.1016/j.cej.2011.11.044

Kumar GVSRP, Komal AM, Yera B, Rao KS (2019) Removal of Cu (II) using three low-cost adsorbents and prediction of adsorption using artificial neural networks. Appl Water Sci 9:1–9. https://doi.org/10.1007/s13201-019-0924-x

Li YH, Ding J, Luan Z, di Z, Zhu Y, Xu C, Wu D, Wei B (2003) Competitive adsorption of Pb2+, Cu2+ and Cd 2+ ions from aqueous solutions by multiwalled carbon nanotubes. Carbon N Y 41: 2787–2792. https://doi.org/10.1016/S0008-6223(03)00392-0

Li H, Xiao DL, He H et al (2013) Adsorption behavior and adsorption mechanism of Cu(II) ions on amino-functionalized magnetic nanoparticles. Trans Nonferrous Met Soc China (English Ed) 23:2657–2665. https://doi.org/10.1016/S1003-6326(13)62782-X

Liu C, Cheng H-M (2005) Carbon nanotubes for clean energy applications. J Phys D Appl Phys 38:R231–R252. https://doi.org/10.1088/0022-3727/38/14/R01

Liu S, Shen Q, Cao Y, Gan L, Wang Z, Steigerwald ML, Guo X (2010) Chemical functionalization of single-walled carbon nanotube field-effect transistors as switches and sensors. Coord Chem Rev 254: 1101–1116. https://doi.org/10.1016/j.ccr.2009.11.007

Liu J, Chen Y, Han T, Cheng M, Zhang W, Long J, Fu X (2019) A biomimetic SiO_2@chitosan composite as highly-efficient adsorbent for removing heavy metal ions in drinking water. Chemosphere 214: 738–742. https://doi.org/10.1016/j.chemosphere.2018.09.172

Liu X, Guan J, Lai G, Xu Q, Bai X, Wang Z, Cui S (2020) Stimuli-responsive adsorption behavior toward heavy metal ions based on comb polymer functionalized magnetic nanoparticles. J Clean Prod 253:119915. https://doi.org/10.1016/j.jclepro.2019.119915

Lu C, Chung YL, Chang KF (2006) Adsorption thermodynamic and kinetic studies of trihalomethanes on multiwalled carbon nanotubes. J Hazard Mater 138:304–310. https://doi.org/10.1016/j.jhazmat.2006.05.076

Lu J, Drzal LT, Worden RM, Lee I (2007) Simple fabrication of a highly sensitive glucose biosensor using enzymes immobilized in exfoliated graphite nanoplatelets nafion membrane. Chem Mater 19:6240–6246. https://doi.org/10.1021/cm702133u

Luo N, Li X, Wang X, Yan H, Zhang C, Wang H (2010) Synthesis and characterization of carbon-encapsulated iron/iron carbide nanoparticles by a detonation method. Carbon N Y 48:3858–3863. https://doi.org/10.1016/j.carbon.2010.06.051

Ma X, Li L, Yang L, Su C, Wang K, Yuan S, Zhou J (2012) Adsorption of heavy metal ions using hierarchical CaCO 3-maltose meso/macroporous hybrid materials: adsorption isotherms and kinetic studies. J Hazard Mater 209–210:467–477. https://doi.org/10.1016/j.jhazmat.2012.01.054

Ma J, Zhuang Y, Yu F (2015) Equilibrium, kinetic and thermodynamic adsorption studies of organic pollutants from aqueous solution onto CNTs/C@Fe/Chitosan composites. New J Chem 39:9299–9305

Machado FM, Fagan SB, da Silva IZ, de Andrade MJ (2015) Carbon nanoadsorbents. In: Carbon nanomaterials as adsorbents for environmental and biological applications, pp 11–32

Mahalingam P, Maiyalagan T, ManiKandan E et al (2013) Dynamic and equilibrium studies on the sorption of basic dye (Basic Brown 4) onto multi-walled carbon nanotubes prepared from renewable carbon precursors. J Environ Nanotechnol 2:43–62. https://doi.org/10.13074/jent.2013.09.132033

Malik LA, Bashir A, Qureashi A, Pandith AH (2019) Detection and removal of heavy metal ions: a review. Environ Chem Lett 17: 1495–1521. https://doi.org/10.1007/s10311-019-00891-z

Marković R, Stevanović J, Stevanović Z et al (2011) Using the low-cost waste materials for heavy metals removal from the mine wastewater. Mater Trans 52:1849–1852. https://doi.org/10.2320/matertrans.M2011191

Maryam M, Suriani AB, Shamsudin MS, Rusop M (2013) BET analysis on carbon nanotubes: comparison between single and double stage thermal CVD method. Adv Mater Res 626:289–293. https://doi.org/10.4028/www.scientific.net/AMR.626.289

Miyamoto JI, Kanoh H, Kaneko K (2005) The addition of mesoporosity to activated carbon fibers by a simple reactivation process. Carbon N Y 43:855–857. https://doi.org/10.1016/j.carbon.2004.10.049

Mubarak NM, Sahu JN, Abdullah EC, Jayakumar NS, Ganesan P (2015) Novel microwave-assisted multiwall carbon nanotubes enhancing Cu (II) adsorption capacity in water. J Taiwan Inst Chem Eng 53: 140–152. https://doi.org/10.1016/j.jtice.2015.02.016

Mubarak NM, Sahu JN, Abdullah EC, Jayakumar NS (2016) Rapid adsorption of toxic Pb(II) ions from aqueous solution using multiwall carbon nanotubes synthesized by microwave chemical vapor deposition technique. J Environ Sci (China) 45:143–155. https://doi.org/10.1016/j.jes.2015.12.025

Nata IF, Wicakso DR, Mirwan A, Irawan C, Ramadhani D, Ursulla (2020) Selective adsorption of Pb(II) ion on amine-rich functionalized rice husk magnetic nanoparticle biocomposites in aqueous solution. J Environ Chem Eng 8:104339. https://doi.org/10.1016/j.jece.2020.104339

Oliveira JA, Cunha FA, Ruotolo LAM (2019) Synthesis of zeolite from sugarcane bagasse fly ash and its application as a low-cost adsorbent to remove heavy metals. J Clean Prod 229:956–963. https://doi.org/10.1016/j.jclepro.2019.05.069

Palanivell P, Ahmed OH, Latifah O, Majid NMA (2020) Adsorption and desorption of nitrogen, phosphorus, potassium, and soil buffering capacity following application of chicken litter biochar to an acid soil. Appl Sci 10:295

Peigney A, Laurent C, Flahaut E, Bacsa RR, Rousset A (2001) Specific surface area of carbon nanotubes and bundles of carbon nanotubes. Carbon N Y 39:507–514. https://doi.org/10.1016/S0008-6223(00)00155-X

Pyrzyńska K, Bystrzejewski M (2010) Comparative study of heavy metal ions sorption onto activated carbon, carbon nanotubes, and carbon-encapsulated magnetic nanoparticles. Colloids Surf A Physicochem Eng Asp 362:102–109. https://doi.org/10.1016/j.colsurfa.2010.03.047

Qu S, Huang F, Yu S, Chen G, Kong J (2008) Magnetic removal of dyes from aqueous solution using multi-walled carbon nanotubes filled with Fe_2O_3 particles. J Hazard Mater 160:643–647. https://doi.org/10.1016/j.jhazmat.2008.03.037

Rafatullah M, Sulaiman O, Hashim R, Ahmad A (2009) Adsorption of copper (II), chromium (III), nickel (II) and lead (II) ions from aqueous solutions by meranti sawdust. J Hazard Mater 170:969–977. https://doi.org/10.1016/j.jhazmat.2009.05.066

Rahman MS, Islam MR (2009) Effects of pH on isotherms modeling for Cu(II) ions adsorption using maple wood sawdust. Chem Eng J 149: 273–280. https://doi.org/10.1016/j.cej.2008.11.029

Rao GP, Lu C, Su F (2007) Sorption of divalent metal ions from aqueous solution by carbon nanotubes: a review. Sep Purif Technol 58:224–231. https://doi.org/10.1016/j.seppur.2006.12.006

Rao MM, Ramana DK, Seshaiah K, Wang MC, Chien SWC (2009) Removal of some metal ions by activated carbon prepared from Phaseolus aureus hulls. J Hazard Mater 166:1006–1013. https://doi.org/10.1016/j.jhazmat.2008.12.002

Rodríguez C, Briano S, Leiva E (2020) Increased adsorption of heavy metal ions in multi-walled carbon nanotubes with improved dispersion stability. Molecules 25:3106

Sankhla MS, Kumari M, Nandan M, Kumar R, Agrawal P (2016) Heavy metals contamination in water and their hazardous effect on human health-a Review. Int J Curr Microbiol Appl Sci 5:759–766. https://doi.org/10.2139/ssrn.3428216

Sengupta J (2018) Carbon nanotube fabrication at industrial scale: opportunities and challenges. In: Handbook of Nanomaterials for Industrial Applications. Elsevier Inc., pp 172–194

Shamsudin MS, Achoi MF, Asiah MN, Ismail LN, Suriani AB, Abdullah S, Yahya SYS, Rusop M (2012, 2012) An investigation on the formation of carbon nanotubes by two-stage chemical vapor deposition. J Nanomater:972126. https://doi.org/10.1155/2012/972126

Shan R, Shi Y, Gu J, Wang Y, Yuan H (2020) Single and competitive adsorption affinity of heavy metals toward peanut shell-derived biochar and its mechanisms in aqueous systems. Chin J Chem Eng 28:1375–1383. https://doi.org/10.1016/j.cjche.2020.02.012

Siddiqa A, Shahid A, Gill R (2015) Silica decorated CNTs sponge for selective removal of toxic contaminants and oil spills from water. J Environ Chem Eng 3:892–897. https://doi.org/10.1016/j.jece.2015.02.026

Sočo E, Kalembkiewicz J (2015) Removal of copper(II) and zinc(II) ions from aqueous solution by chemical treatment of coal fly ash. Croat Chem Acta 88:267–279. https://doi.org/10.5562/cca2646

Sun WL, Xia J, Shan YC (2014) Comparison kinetics studies of Cu(II) adsorption by multi-walled carbon nanotubes in homo and heterogeneous systems: effect of nano-SiO_2. Chem Eng J 250:119–127. https://doi.org/10.1016/j.cej.2014.03.094

Suriani AB, Azira AA, Nik SF, Md Nor R, Rusop M (2009) Synthesis of vertically aligned carbon nanotubes using natural palm oil as carbon precursor. Mater Lett 63:2704–2706. https://doi.org/10.1016/j.matlet.2009.09.048

Suriani AB, Nor RM, Rusop M (2010) Vertically aligned carbon nanotubes synthesized from waste cooking palm oil. J Ceram Soc Jpn 65–66:963–968. https://doi.org/10.2109/jcersj2.118.963

Suriani AB, Dalila AR, Mohamed A, Mamat MH, Salina M, Rosmi MS, Rosly J, Md Nor R, Rusop M (2013) Vertically aligned carbon nanotubes synthesized from waste chicken fat. Mater Lett 101:61–64. https://doi.org/10.1016/j.matlet.2013.03.075

Suriani AB, Alfarisa S, Mohamed A, Isa IM, Kamari A, Hashim N, Mamat MH, Mohamed AR, Rusop M (2015a) Quasi-aligned carbon nanotubes synthesised from waste engine oil. Mater Lett 139:220–223. https://doi.org/10.1016/j.matlet.2014.10.046

Suriani AB, Dalila AR, Mohamed A, Soga T, Tanemura M (2015b) Synthesis, structural, and field electron emission properties of quasi-aligned carbon nanotubes from gutter oil. Mater Chem Phys 165:1–7. https://doi.org/10.1016/j.matchemphys.2015.09.002

Suriani AB, Safitri RN, Mohamed A, Alfarisa S, Isa IM, Kamari A, Hashim N, Ahmad MK, Malek MF, Rusop M (2015c) Enhanced field electron emission of flower-like zinc oxide on zinc oxide nanorods grown on carbon nanotubes. Mater Lett 149:66–69. https://doi.org/10.1016/j.matlet.2015.02.115

Suriani AB, Dalila AR, Mohamed A, Mamat MH, Malek MF, Soga T, Tanemura M (2016a) Fabrication of vertically aligned carbon nanotubes-zinc oxide nanocomposites and their field electron emission enhancement. Mater Des 90:185–195. https://doi.org/10.1016/j.matdes.2015.10.051

Suriani AB, Norhafizah J, Mohamed A, Mamat MH, Malek MF, Ahmad MK (2016b) Scaled-up prototype of carbon nanotube production system utilizing waste cooking palm oil precursor and its nanocomposite application as supercapacitor electrodes. J Mater Sci Mater Electron 27:11599–11605. https://doi.org/10.1007/s10854-016-5291-x

Suriani AB, Safitri RN, Mohamed A, Alfarisa S, Malek MF, Mamat MH, Ahmad MK (2016c) Synthesis and field electron emission properties of waste cooking palm oil-based carbon nanotubes coated on different zinc oxide nanostructures. J Alloys Compd 656:368–377. https://doi.org/10.1016/j.jallcom.2015.09.277

Tang WW, Zeng GM, Gong JL, Liu Y, Wang XY, Liu YY, Liu ZF, Chen L, Zhang XR, Tu DZ (2012) Simultaneous adsorption of atrazine and Cu (II) from wastewater by magnetic multi-walled carbon nanotube. Chem Eng J 211–212:470–478. https://doi.org/10.1016/j.cej.2012.09.102

Tofighy MA, Mohammadi T (2011) Adsorption of divalent heavy metal ions from water using carbon nanotube sheets. J Hazard Mater 185:140–147. https://doi.org/10.1016/j.jhazmat.2010.09.008

Van Thuan T, Quynh BTP, Nguyen TD et al (2017) Response surface methodology approach for optimization of Cu2+, Ni2+ and Pb2+ adsorption using KOH-activated carbon from banana peel. Surf Interfaces 6:209–217. https://doi.org/10.1016/j.surfin.2016.10.007

Vázquez OFG, del Rosario Moreno V, Hernández Montoya V et al (2016) Adsorption of heavy metals in the presence of a magnetic field on adsorbents with different magnetic properties. Ind Eng Chem Res 55:9323–9331. https://doi.org/10.1021/acs.iecr.6b01990

Vuković GD, Marinković AD, Čolić M, Ristić MĐ, Aleksić R, Perić-Grujić AA, Uskoković PS (2010) Removal of cadmium from aqueous solutions by oxidized and ethylenediamine-functionalized multi-walled carbon nanotubes. Chem Eng J 157:238–248. https://doi.org/10.1016/j.cej.2009.11.026

Wadhawan S, Jain A, Nayyar J, Mehta SK (2020) Role of nanomaterials as adsorbents in heavy metal ion removal from waste water: a review. J Water Process Eng 33:101038. https://doi.org/10.1016/j.jwpe.2019.101038

Wang H, Yan N, Li Y, Zhou X, Chen J, Yu B, Gong M, Chen Q (2012) Fe nanoparticle-functionalized multi-walled carbon nanotubes: one-pot synthesis and their applications in magnetic removal of heavy metal ions. J Mater Chem 22:9230–9236. https://doi.org/10.1039/c2jm16584h

Wang J, Li Z, Li S, Qi W, Liu P, Liu F, Ye Y, Wu L, Wang L, Wu W (2013) Adsorption of Cu(II) on oxidized multi-walled carbon nanotubes in the presence of hydroxylated and carboxylated fullerenes. PLoS One 8:1–11. https://doi.org/10.1371/journal.pone.0072475

Wright AC, Faulkner MK, Harris RC, Goddard A, Abbott AP (2012) Nanomagnetic domains of chromium deposited on vertically-aligned carbon nanotubes. J Magn Magn Mater 324:4170–4174. https://doi.org/10.1016/j.jmmm.2012.07.044

Yadav DK, Srivastava S (2017) Carbon nanotubes as adsorbent to remove heavy metal ion (Mn + 7) in wastewater treatment. Mater Today Proc 4:4089–4094. https://doi.org/10.1016/j.matpr.2017.02.312

Yusoff SNM, Kamari A, Putra WP, Ishak CF, Mohamed A, Hashim N, Isa IM (2014) Removal of Cu(II), Pb(II) and Zn(II) ions from aqueous solutions using selected agricultural wastes: adsorption and characterisation studies. J Environ Prot (Irvine, Calif) 05:289–300. https://doi.org/10.4236/jep.2014.54032

Zare K, Gupta VK, Moradi O, Makhlouf ASH, Sillanpää M, Nadagouda MN, Sadegh H, Shahryari-ghoshekandi R, Pal A, Wang ZJ, Tyagi I, Kazemi M (2015) A comparative study on the basis of adsorption capacity between CNTs and activated carbon as adsorbents for removal of noxious synthetic dyes: a review. J Nanostruct Chem 5:227–236. https://doi.org/10.1007/s40097-015-0158-x

Zhuang Y, Liu J, Chen J, Fei P (2020) Food and Bioproducts Processing Modified pineapple bran cellulose by potassium permanganate as a copper ion adsorbent and its adsorption kinetic and adsorption thermodynamic. Food Bioprod Process 122:82–88. https://doi.org/10.1016/j.fbp.2020.04.008